

# High-performance sampling of generic Determinantal Point Processes

Jack Poulson\*

August 20, 2019

## Abstract

Determinantal Point Processes (DPPs) were introduced by Macchi [1] as a model for repulsive (fermionic) particle distributions. But their recent popularization is largely due to their usefulness for encouraging diversity in the final stage of a recommender system [2].

The standard sampling scheme for finite DPPs is a spectral decomposition followed by an equivalent of a randomly diagonally-pivoted Cholesky factorization of an orthogonal projection, which is only applicable to Hermitian kernels and has an expensive setup cost. Researchers [3, 4] have begun to connect DPP sampling to  $LDL^H$  factorizations as a means of avoiding the initial spectral decomposition, but existing approaches have only outperformed the spectral decomposition approach in special circumstances, where the number of kept modes is a small percentage of the ground set size.

This article proves that trivial modifications of  $LU$  and  $LDL^H$  factorizations yield efficient direct sampling schemes for non-Hermitian and Hermitian DPP kernels, respectively. Further, it is experimentally shown that even dynamically-scheduled, shared-memory parallelizations of high-performance dense and sparse-direct factorizations can be trivially modified to yield DPP sampling schemes with essentially identical performance.

The software developed as part of this research, Catamari [hodgestar.com/catamari] is released under the Mozilla Public License v2.0. It contains header-only, C++14 plus OpenMP 4.0 implementations of dense and sparse-direct, Hermitian and non-Hermitian DPP samplers.

---

\*jack@hodgestar.com, Hodge Star Scientific Computing

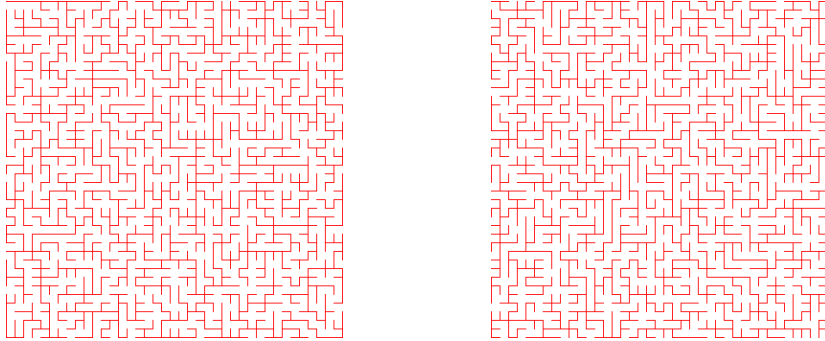


Figure 1: Two samples from the uniform distribution over spanning trees of a  $40 \times 40$  box of  $\mathbb{Z}^2$ . Each has likelihood  $\exp(-1794.24)$ .

## 1 Introduction

Determinantal Point Processes (DPPs) were first studied as a distinct class by Macchi in the mid 1970's [1, 5] as a probability distribution for the locations of repulsive (fermionic) particles, in direct contrast with Permanent – or, bosonic – Point Processes. Particular instances of DPPs, representing the eigenvalue distributions of classical random matrix ensembles, appeared in a series of papers in the beginning of the 1960's [6, 7, 8, 9, 10] (see [11] for a review, and [12] for a computational perspective on sampling classical eigenvalue distributions). Some of the early investigations of (finite) DPPs involved their usage for uniformly sampling spanning trees of graphs [13, 14] (see Figs. 1 and 2), non-intersecting random walks [15], and domino tilings of the Aztec diamond [16, 17, 18, 19] (see Figs. 3 and 4).

Let us recall that the class of *immanants* provides a generalization of the determinant and permanent of a matrix by using an arbitrary character  $\chi$  of the symmetric group  $S_n$  to determine the signs of terms in the summation:

$$|A|^\chi \equiv \sum_{\sigma \in S_n} \chi(\sigma) \prod_{i=1}^n A_{i, \sigma(i)}.$$

Choosing the trivial character  $\chi \equiv 1$  yields the permanent, while choosing  $\chi(\sigma) = \text{sign}(\sigma)$  provides the determinant. The resulting generalization from Determinantal Point Processes and Permanent Point Processes to Immanantal Point Processes was studied in [20].

### Definition 1

A *finite Determinantal Point Process* is a random variable  $\mathbf{Y} \sim \text{DPP}(K)$

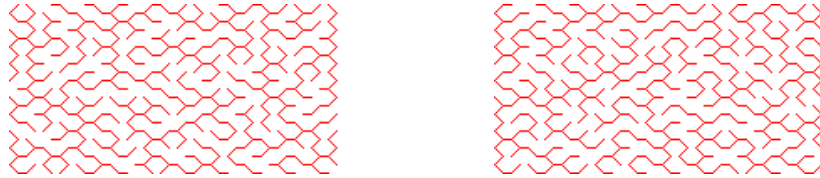


Figure 2: Two samples from the uniform distribution over spanning trees of a 10 x 10 section of hexagonal tiles. Each has likelihood  $\exp(-299.101)$ .

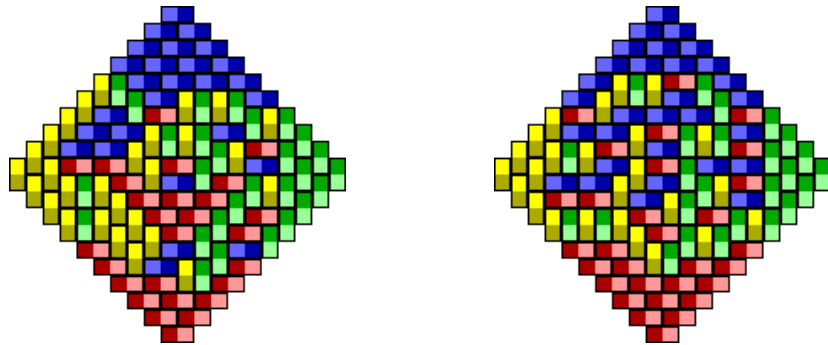


Figure 3: Two samples from the Aztec diamond DPP of order 10, defined via a complex, non-Hermitian kernel based upon Kenyon's formula over the Kasteleyn matrix. The tiles all begin on dark squares and are oriented either: left (blue), right (red), up (yellow), or down (green). Their likelihoods are both  $\exp(-38.1231)$ .

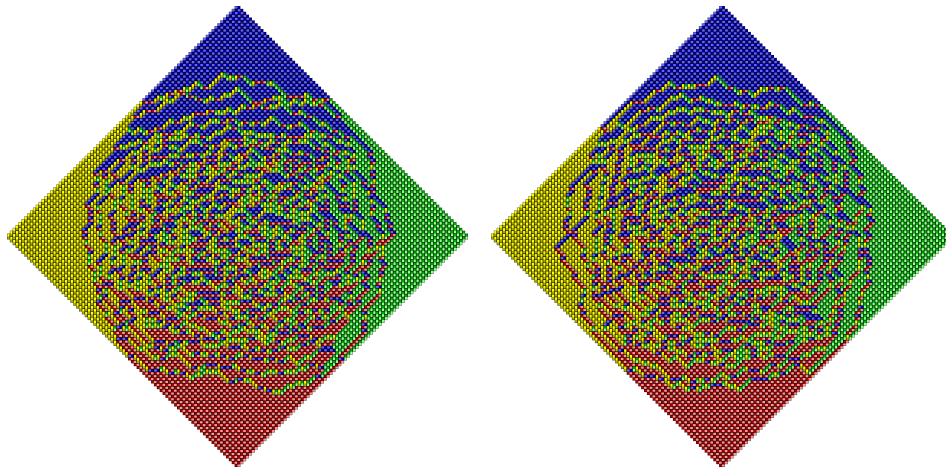


Figure 4: Two samples from the Aztec diamond DPP of order 80, defined via a complex, non-Hermitian kernel based upon Kenyon’s formula over the Kasteleyn matrix. Their likelihoods are both  $\exp(-2245.8)$ . The diamond is large enough to clearly display the *arctic circle* phenomenon discussed in [21] and [19]: “when  $n$  is sufficiently large, the shape of the central sub-region becomes arbitrarily close to a perfect circle of radius  $n/\sqrt{2}$  for all but a negligible proportion of the tilings.”

over the power set of a ground set  $\{0, 1, \dots, n-1\} = [n]$  such that

$$\mathbb{P}[Y \subseteq \mathbf{Y}] = \det(K_Y),$$

where  $K \in \mathbb{C}^{n \times n}$  is called the **marginal kernel matrix** and  $K_Y$  denotes the restriction of  $K$  to the row and column indices of  $Y$ .

We can immediately observe that the  $j$ -th diagonal entry of a marginal kernel  $K$  is the probability of index  $j$  being in the sample,  $\mathbf{Y}$ , so the diagonal of every marginal kernel must lie in  $[0, 1] \subset \mathbb{R}$ . A characteristic requirement for a complex matrix to be admissible as a marginal kernel is given in the following proposition, due to Brunel [22], which we will provide an alternative proof of after introducing our factorization-based sampling algorithm.

**Proposition 1** (Brunel [22])

A matrix  $K \in \mathbb{C}^{n \times n}$  is admissible as a DPP marginal kernel iff

$$(-1)^{|J|} \det(K - \mathbf{1}_J) \geq 0, \quad \forall J \subseteq [n].$$

We can also observe that, because determinants are preserved under similarity transformations, there is a nontrivial equivalence class for marginal kernels – which is to say, there are many marginal kernels defining the same DPP:

**Proposition 2**

The equivalence class of a DPP kernel  $K \in \mathbb{C}^{n \times n}$  contains its orbit under the group of diagonal similarity transformations, i.e.,

$$\{D^{-1}KD : D = \text{diag}(d), d \in (\mathbb{C} \setminus \{0\})^n\}.$$

If we restrict to the classes of complex Hermitian or real symmetric kernels, the same statement holds with the entries of  $d$  restricted to the circle group  $U(1) = \{z \in (\mathbb{C}, \times) : |z| = 1\}$  and the scalar orthogonal group  $O(1) = \{z \in (\mathbb{R}, \times) : |z| = 1\}$ , respectively.

*Proof.* Determinants are preserved under similarity transformations, so the probability of inclusion of each subset is unchanged by global diagonal similarity. That a unitary diagonal similarity preserves Hermiticity follows from recognition that it becomes a Hermitian congruence. Likewise, a signature matrix similarity transformation becomes a real symmetric congruence.  $\square$

In most works, with the notable exception of Kasteleyn matrix approaches to studying domino tilings of the Aztec diamond [16, 17, 18, 19], the

marginal kernel is assumed Hermitian. And Macchi [1] showed (Cf. [23, 24]) that a Hermitian matrix is admissible as a marginal kernel if and only if its eigenvalues all lie in  $[0, 1]$ . The viewpoint of these eigenvalues as probabilities turns out to be productive, as the most common sampling algorithm for Hermitian DPPs, due to [24] and popularized in the machine learning community by [2], produces an equivalent random orthogonal projection matrix by preserving eigenvectors with probability equal to their eigenvalue:

**Theorem 1** (Theorem 7 of [24])

*Given any Hermitian marginal kernel matrix  $K \in \mathbb{C}^{n \times n}$  with spectral decomposition  $Q\Lambda Q^H$ , sampling from  $\mathbf{Y} \sim \text{DPP}(K)$  is equivalent to sampling from a realization of the random DPP with kernel  $Q_{:, \mathbf{Z}} Q_{:, \mathbf{Z}}^H$ , where  $Q_{:, \mathbf{Z}}$  consists of the columns of  $Q$  with  $\mathbb{P}[j \in \mathbf{Z}] = \Lambda_j$ , independently for each  $j$ .*

Such an orthogonal projection marginal kernel is said to define a **Determinantal Projection Process** [24], or **elementary DPP** [2], and it is known that the resulting samples almost surely have cardinality equal to the rank of the projection (e.g., Lemma 17 of [24]). The algebraic specification in Alg. 1 of [2] of the Alg. 18 of [24] involved an  $O(nk^3)$  approach, where  $k$  is the rank of the projection kernel. In many important cases, such as uniformly sampling spanning trees or domino tilings,  $k$  is a large fraction of  $n$ , and the algorithm has quartic complexity (assuming standard matrix multiplication). In the words of [2]:

Alg. 1 runs in time  $O(nk^3)$ , where  $k$  is the number of eigenvectors selected [...] the initial eigendecomposition [...] is often the computational bottleneck, requiring  $O(n^3)$  time. Modern multi-core machines can compute eigendecompositions up to  $n \approx 1,000$  at interactive speeds of a few seconds, or larger problems up to  $n \approx 10,000$  in around ten minutes.

A faster,  $O(nk^2)$  algorithm for sampling elementary DPPs was given as Alg. 2 of [25]. We will later show that this approach is equivalent to a small modification of a diagonally-pivoted, rank-revealing, left-looking, Cholesky factorization [26], where the pivot index is chosen at each iteration by sampling from the probability distribution implied by the diagonal of the remaining submatrix (which is maintained out-of-place).

As a brief aside, we recall that the distinction between *up-looking*, *left-looking*, and *right-looking* factorizations is based upon their choice of loop invariant. Given the matrix partitioning

$$\begin{pmatrix} A_{1,1} & A_{1,2} \\ A_{2,1} & A_{2,2} \end{pmatrix},$$

where the diagonal of  $A_{1,1}$  comprises the list of eliminated pivots: an *up-looking* algorithm will have only updated  $A_{1,1}$  (by overwriting it with its factorization), a *left-looking* algorithm will also have overwritten  $A_{2,1}$  with the corresponding block column of the lower triangular factor (and  $A_{1,2}$  with its upper-triangular factor in the nonsymmetric case), and a *right-looking* algorithm will additionally have overwritten  $A_{2,2}$  with the Schur complement resulting from the block elimination of  $A_{1,1}$ .

Researchers have begun proposing algorithms which directly sample from Hermitian marginal kernels by sequentially deciding whether each index should be in the result by sampling the Bernoulli process defined by the probability of the item’s inclusion, conditioned on the combination of all of the explicit inclusion and exclusion decisions made so far. For example, when deciding whether to include index  $j$  in the sample, we will have already partitioned  $[0, \dots, j-1]$  into a set of included indices,  $F$ , and excluded indices,  $G$ . So we must sample index  $j$  with probability  $\mathbb{P}[j \in \mathbf{Y} \mid F \subseteq \mathbf{Y}, G \cap \mathbf{Y} = \emptyset]$ . Directly performing such sampling using formulae for marginal kernels of conditional DPPs is referred to in [3] as *sequential sampling* (Cf. [4] for greedy, maximum-likelihood inference).

The primary contribution of this manuscript is to show that sequential sampling can be performed via a small modification of an unpivoted  $LDL^H$  factorization process (where  $L$  is unit lower-triangular and  $D$  is real diagonal) and to extend them to non-Hermitian marginal kernels using an unpivoted  $LU$  factorization; [27] motivates an algorithm for learning non-Hermitian DPP kernels by their ability to incorporate both attraction and repulsion between items.

It is then demonstrated that high-performance factorizations techniques [28, 29, 30] lead to orders of magnitude accelerations, and that sparse-direct techniques [31, 32, 33] can yield further orders of magnitude speedups.

## 2 Prototype factorization-based DPP sampling

To describe factorization processes, we will extend our earlier notation that, for an  $n \times n$  matrix  $K$  and an index subset  $Y \subseteq [n]$ ,  $K_Y$  refers to the restriction of  $K$  to the row and column indices of  $Y$ . Given a second index subset  $Z \subseteq [n]$ ,  $K_{Y,Z}$  will denote the restriction of  $K$  to the  $|Y| \times |Z|$  submatrix consisting of the rows indices in  $Y$  and the column indices in  $Z$ . And we use the notation  $[j : k]$  to represent the integer range  $\{j, j+1, \dots, k-1\}$ .

Our derivation will make use of a few elementary propositions on the

forms of marginal kernels for conditional DPPs. These propositions will allow us to define modifications to the pivots of an LU factorization so that the resulting Schur complements correspond to the marginal kernel of the DPP over the remaining indices, conditioned on the inclusion decisions of the indices corresponding to the eliminated pivots.

**Proposition 3**

Given disjoint subsets  $A, B \subseteq [n]$  of the ground set of a DPP with marginal kernel  $K$ , almost surely

$$\mathbb{P}[B \subseteq \mathbf{Y} | A \subseteq \mathbf{Y}] = \det(K_B - K_{B,A}K_A^{-1}K_{A,B}).$$

*Proof.* If  $A \subseteq \mathbf{Y}$ , then  $\det(K_A) = \mathbb{P}[A \subseteq \mathbf{Y}] > 0$  almost surely, so we may perform a two-by-two block LU decomposition

$$\begin{pmatrix} K_A & K_{A,B} \\ K_{B,A} & K_B \end{pmatrix} = \begin{pmatrix} I & 0 \\ K_{B,A}K_A^{-1} & K_B - K_{B,A}K_A^{-1}K_{A,B} \end{pmatrix} \begin{pmatrix} K_A & K_{A,B} \\ 0 & I \end{pmatrix}.$$

That  $\det : GL(n, \mathbb{C}) \mapsto (\mathbb{C}, \times)$  is a homomorphism yields

$$\det(K_{A \cup B}) = \det(K_A) \det(K_B - K_{B,A}K_A^{-1}K_{A,B}).$$

The result then follows from the definition of conditional probabilities for a DPP:

$$\mathbb{P}[B \subseteq \mathbf{Y} | A \subseteq \mathbf{Y}] = \frac{\mathbb{P}[A, B \subseteq \mathbf{Y}]}{\mathbb{P}[A \subseteq \mathbf{Y}]} = \frac{\det(K_{A \cup B})}{\det(K_A)}.$$

□

**Proposition 4**

Given disjoint  $a \in [n]$  and  $B \subset [n]$  for a ground set  $[n]$  of a DPP with marginal kernel  $K$ , almost surely

$$\mathbb{P}[B \subset \mathbf{Y} | a \notin \mathbf{Y}] = \det(K_B - K_{B,a}(K_a - 1)^{-1}K_{a,B}).$$

*Proof.*

$$\begin{aligned} \mathbb{P}[B \subset \mathbf{Y} | a \notin \mathbf{Y}] &= \frac{\mathbb{P}[a \notin \mathbf{Y} | B \subset \mathbf{Y}] \mathbb{P}[B \subset \mathbf{Y}]}{\mathbb{P}[a \notin \mathbf{Y}]} \\ &= \frac{(1 - \mathbb{P}[a \in \mathbf{Y} | B \subset \mathbf{Y}]) \mathbb{P}[B \subset \mathbf{Y}]}{1 - \mathbb{P}[a \in \mathbf{Y}]} \\ &= \frac{\det(K_B) - \det(K_{a \cup B})}{1 - K_a} \\ &= \det(K_B) \left(1 - K_{a,B} \frac{K_B^{-1}}{K_a - 1} K_{B,a}\right) \\ &= \det(K_B - K_{B,a}(K_a - 1)^{-1}K_{a,B}), \end{aligned}$$

where the last equality makes use of the Matrix Determinant Lemma. The formulae are well-defined almost surely.  $\square$

Propositions 3 and 4 are enough to derive our direct, non-Hermitian DPP sampling algorithm. But, for the sake of symmetry with Proposition 3, we first generalize to set exclusion:

**Proposition 5**

*Given disjoint subsets  $A, B \subset \mathcal{Y}$ , almost surely*

$$\mathbb{P}[B \subseteq \mathbf{Y} | A \subseteq \mathbf{Y}^c] = \det(K_B - K_{B,A}(K_A - I)^{-1}K_{A,B}).$$

*Proof.* The claim follows from recursive formulation of conditional marginal kernels using the previous proposition. The resulting kernel is equivalent to the Schur complement produced from the block LU factorization

$$\begin{pmatrix} K_A - I & K_{A,B} \\ K_{B,A} & K_B \end{pmatrix} = \begin{pmatrix} I & 0 \\ K_{B,A}(K_A - I)^{-1} & K_B - K_{B,A}(K_A - I)^{-1}K_{A,B} \end{pmatrix} \begin{pmatrix} K_A - I & K_{A,B} \\ 0 & I \end{pmatrix},$$

as the subtraction of 1 from each eliminated pivot commutes with the outer product updates.  $\square$

**Theorem 2** (Factorization-based DPP sampling)

*Given a (possibly non-Hermitian) marginal kernel matrix  $K$  of order  $n$ , an LU factorization of  $K$  can be modified as in Algorithm 1 to almost surely provide a sample from  $DPP(K)$ . This algorithm involves roughly  $\frac{2}{3}n^3$  floating-point operations, and the likelihood of any returned sample will be given by the product of the absolute value of the diagonal of the result. If the marginal kernel is Hermitian, the work can be roughly halved by exploiting symmetry in the Schur complement updates.*

*Proof.* We first demonstrate, by induction, that our factorization algorithm samples the DPP generated by the marginal kernel  $K$ . The loop invariant is that, at the start of the iteration for pivot index  $j$ ,  $A_{[j:n]}$  represents the equivalence class of kernels for the DPP over indices  $[j : n]$  conditioned on the inclusion decisions for indices  $0, \dots, j - 1$ .

Since the diagonal entries of a kernel matrix represent the likelihood of the corresponding index being in the sample, the loop invariant implies that index  $j$  is kept with the correct conditional probability. Prop. 3 shows that the loop invariant is almost surely maintained when the Bernoulli draw is successful, and Prop. 4 handles the alternative. Thus, the loop invariant holds almost surely, and, upon completion, the proposed algorithm samples each subset with the correct probability by sequentially iterating over

Algorithm 1: Unblocked, right-looking, non-Hermitian DPP sampling. For a sample  $Y$ , the returned matrix  $A$  will contain the in-place  $LU$  factorization of  $K - \mathbb{1}_{Y^C}$ , where  $\mathbb{1}_{Y^C}$  is the diagonal indicator matrix for the entries not in the sample. Symmetry can be exploited in the outer products when the kernel is Hermitian.

```

1 sample := []; A := K
2 for j in range(n):
3     sample.append(j) if Bernoulli(Aj) else Aj -= 1
4     A[j+1:n],j /= Aj
5     A[j+1:n] -= A[j+1:n],j Aj,[j+1:n]
6 return sample, A

```

each index, making an inclusion decision with the appropriate conditional probability.

The likelihood of a sample produced by the algorithm is thus the product of the likelihoods of the results of the Bernoulli draws: when a draw for a diagonal entry  $p_j$  is successful, its probability was  $p_j$ , and, when unsuccessful,  $1 - p_j$ . In both cases, the multiplicative contribution is the absolute value of the final state of the  $j$ 'th diagonal entry.  $\square$

Theorem 2 provides us with another interpretation of the generic DPP kernel admissibility condition of [22]:

*Proposition 1 above.* When Algorithm 1 produces a sample  $Y$ , the resulting upper and strictly-lower triangular portions of the resulting matrix respectively contain the  $U$  and strictly-lower portion of the unit-diagonal  $L$  from the LU factorization of  $K - \mathbb{1}_{Y^C}$ . And we have:

$$\det(K - \mathbb{1}_{Y^C}) = \det(U) = \prod_{j=0}^{n-1} U_j = \prod_{j \in Y} p_j \prod_{j \in Y^C} (p_j - 1),$$

where  $p_j$  is the inclusion probability for index  $j$ , conditioned on the inclusion decisions of indices  $0, \dots, j - 1$ .

One can inductively show, working backwards from the last pivot, that  $(-1)^{|Y^C|} \det(K - \mathbb{1}_{Y^C})$  always being non-negative is equivalent to all potential pivots produced by our sampling algorithm, the set of conditional inclusion probabilities, living in  $[0, 1]$ . Otherwise, there would exist an index inclusion decision change which would not change the sign of  $\det(K - \mathbb{1}_{Y^C})$ .  $\square$

By replacing the Bernoulli samples of algorithm 2 with the maximum-likelihood result for each index inclusion, we arrive at an analogous (approximate) maximum-likelihood inference algorithm.

In both cases, the same specializations that exist for modifying an unpivoted LU factorization into a Cholesky or (unpivoted)  $LDL^H$  or  $LDL^T$  factorization apply to our DPP sampling algorithms. And as we will see in the next two sections, so do high-performance dense and sparse-direct factorization techniques.

As a brief aside, for real matrices, assuming standard matrix multiplication algorithms, the highest-order terms for the operation counts of dense Gaussian Elimination and an MRRR-based [34] Hermitian eigensolver are  $\frac{2}{3}n^3$  and  $\frac{10}{3}n^3$  [35]. But the coefficient for the Hermitian eigensolver is misleadingly small, as the initial phase of a Hermitian eigensolver traditionally involves a unitary reduction to Hermitian tridiagonal form that, due to only modest potential for data reuse, executes significantly less efficiently than traditional dense factorizations. So-called Successive Band Reduction techniques [36, 37, 38] were therefore introduced as a gambit for trading higher operation counts for decreased data movement and – as a consequence – increased performance.

**Theorem 3** (Factorization-based elementary DPP sampling)

*Given a marginal kernel matrix  $K$  of order  $n$  which is an orthogonal projection of rank  $k$ , performing  $k$  steps of diagonally-pivoted Cholesky factorization, where each pivot index is chosen by sampling from the diagonal as in Algorithm 2, is equivalent to sampling from  $DPP(K)$ . This approach has complexity  $O(nk^2)$  and almost surely completes and returns a sample of cardinality  $k$ ; the likelihood of the resulting sample is the square of the product of the first  $k$  diagonal entries of the partially factored matrix.*

*Proof.* Alg. 2 is, up to permutation, algebraically equivalent to the sampling phase of Alg. 2 of [25]: for the sake of simplicity, it assumes the Gramian is preformed rather than forming it on the fly from the factor. That the probability of a cardinality  $k$  sample  $Y$  is, almost surely, equal to the product of the squares of the first  $k$  diagonal entries of the result follows from recognizing that the lower triangle of the top-left  $k \times k$  submatrix will be the Cholesky factor of  $K_Y$ , and

$$\mathbb{P}[Y = \mathbf{Y}] = \mathbb{P}[Y \subseteq \mathbf{Y}] = \det(K_Y) = \det(L_Y L_Y^H) = \det(L_Y) \det(L_Y^H) = \prod_{j=0}^{k-1} A_j^2.$$

□

Algorithm 2: Unblocked, left-looking, diagonally-pivoted, Cholesky-based sampling of a Hermitian Determinantal Projection Process. For a sample  $Y$ , the returned matrix will contain the in-place Cholesky factorization of  $K_Y$ . The computational cost is  $O(nk^2)$ .

```

1  $A \Leftarrow K$ ;  $d \Leftarrow \text{diag}(K)$ ; orig_indices := [0:n]
2 for j in range(k):
3     # Sample pivot index and permute
4     Draw index t from [j:n] with probability  $d_t/(k-j)$ 
5     Perform Hermitian swap of indices j and t of A
6     Swap positions j and t of orig_indices and d
7      $A_j := \sqrt{d_j}$ 
8     if j == k - 1:
9         break
10    # Form new column and update diagonal
11     $A_{[j+1:n],j} \Leftarrow A_{[j+1:n],[0:j]} A_{j,[0:j]}^H$ 
12    for t in range(j+1, n):
13         $A_{t,j} \Leftarrow A_j$ 
14         $d_t \Leftarrow |A_{t,j}|^2$ 
15 return orig_indices [0:k],  $A_{[0:k]}$ 

```

The permutations in Alg. 2 were introduced to solidify the connection to a traditional diagonally-pivoted Cholesky factorization. There is the additional benefit of simplifying the usage of Basic Linear Algebra Subprograms (BLAS) [39, 40, 41] calls for the matrix/vector products. But the bulk of the work of this approach will be in rank-one updates, which have essentially no data reuse, and are therefore not performant on modern machines, where the peak floating-point performance is substantially faster than what can be read directly from main memory. The Linear Algebra PACKage (LAPACK) [28] was introduced in 1990 as proof that dense factorizations can be recast in terms of matrix/matrix multiplications; we present analogues in the following section, as well as multi-core, tiled extensions similar to [29, 30].

### 3 High-performance, dense, factorization-based DPP sampling

The main idea of LAPACK [28] is to reorganize the computations within dense linear algebra algorithms so that as much of the work as possible is recast into composing matrices with nontrivial minimal dimensions. Basic operations rich in such matrix compositions – typically referred to as *Level 3 BLAS* [41] – are the building blocks of LAPACK. In most cases, such *block sizes* range from roughly 32 to 256, with 64 to 128 being most common.

In the case of triangular factorizations, such as Cholesky,  $LDL^H$ , and LU, a *blocked* algorithm can be produced from the unblocked algorithm by carefully matricizing each of the original operations. In the case of a right-looking LU factorization without pivoting, one arrives at Alg. 3, where  $A_{J_1}$  takes the place of the scalar pivot and must be factored – typically, using the unblocked algorithm being generalized – before its components are used to solve against  $A_{J_2, J_1}$  and  $A_{J_1, J_2}$ .

Algorithm 3: Blocked LU factorization without pivoting. The functions `triu` and `unit_tril` mirror MATLAB notation and respectively return the upper-triangular and unit-diagonal lower-triangular restrictions of their input matrices.

```

1 | j := 0
2 | while j < n:
3 |   bsize := min(blocksize, n - j)
4 |   J1 = [j : j + bsize]; J2 = [j + bsize : n]
```

```

5    $A_{J_1} = \text{unblocked\_lu}(A_{J_1})$ 
6    $A_{J_2, J_1} := A_{J_2, J_1} \text{triu}(A_{J_1})^{-1}$ 
7    $A_{J_1, J_2} := \text{unit\_tril}(A_{J_1})^{-1} A_{J_1, J_2}$ 
8    $A_{J_2} -= A_{J_2, J_1} A_{J_1, J_2}$ 
9    $j += \text{bsize}$ 
10  return sample , A

```

The correct form of these solves can be derived via the relationship:

$$\begin{pmatrix} A_1 & A_{1,2} \\ A_{2,1} & A_2 \end{pmatrix} = \begin{pmatrix} L_1 & 0 \\ L_{2,1} & L_2 \end{pmatrix} \begin{pmatrix} U_1 & U_{1,2} \\ 0 & U_2 \end{pmatrix} = \begin{pmatrix} L_1 U_1 & L_1 U_{1,2} \\ L_{2,1} U_1 & L_{2,1} U_{1,2} + L_2 U_2 \end{pmatrix},$$

where we used shorthand of the form  $A_{1,2}$  to represent  $A_{J_1, J_2}$ . An unblocked factorization can be used to compute the triangular factors  $L_1$  and  $U_1$  of the diagonal block  $A_1$ , and then triangular solves of the form  $L_{2,1} := A_{2,1} U_1^{-1}$  and  $U_{1,2} := L_1^{-1} A_{1,2}$  yield the two panels. After forming the Schur complement  $S_2 := A_2 - L_{2,1} U_{1,2}$ , the problem has been reduced to an LU factorization with fewer variables – that of  $L_2 U_2 = S_2$ . Asymptotically, all of the work is performed in the outer-product updates which form the Schur complements.

The conversion of Alg. 1, an unblocked DPP sampler, into Alg. 4, a blocked DPP sampler, is essentially identical to the formulation of Alg. 3 from an unblocked LU factorization. We emphasize that, while it is well-known that  $LU$  factorizations without pivoting fail on large classes of nonsingular matrices – for example, any matrix with a zero in the top-left position – the analogue for DPP sampling succeeds almost surely for any marginal kernel.

Algorithm 4: Blocked, factorization-based, non-Hermitian DPP sampling. For a sample  $Y$ , the returned matrix  $A$  will contain the in-place  $LU$  factorization of  $K - \mathbb{1}_{Y^c}$ , where  $\mathbb{1}_{Y^c}$  is the diagonal indicator matrix for the entries not in the sample,  $\mathbf{Y}$ . The usual specializations from  $LU$  to  $LDL^H$  factorization applies if the kernel is Hermitian.

```

1   sample := []; A := K; j := 0
2   Replace line 5 of main loop of Alg. 3 with:
3     subsample,  $A_{J_1} = \text{unblocked\_dpp}(A_{J_1})$ 
4     sample.append(subsample + j)

```

```
5 | return sample , A
```

Beyond the order-of-magnitude improvement provided by such algorithms, even on a single core of a modern computer, they also simplify the incorporation of parallelism. Lifting algorithms into blocked form allows for each core to be dynamically assigned tasks corresponding to individual updates of a *tile* [29, 30], a roughly `tile_size`  $\times$  `tile_size` submatrix which, in our experiments, was typically most performant for `tile_size` = 256.

Within the context of Alg. 4, our tiled algorithm assigns each `unblocked_dpp` call an individual OpenMP 4.0 [42] task which depends upon the last Schur complement update of its tile. The triangular solves against  $U_{J_1}$  are split into submatrices mostly of the form `tile_size`  $\times$  `block_size`, those of the solves against  $L_{J_1}$  are roughly of the transpose dimensions, while the Schur complement tasks are roughly of size `tile_size`  $\times$  `tile_size`. In each case, tile reads and writes are scheduled using dependencies on previous updates of the same tile.

The performance of such a dynamically-scheduled parallelization of the Hermitian specialization of Alg. 4 is demonstrated for arbitrary dense, Hermitian marginal kernels on a 16-core Intel i9-7960x in Fig. 5. The performance of a similarly parallelized unpivoted  $LDL^H$  factorization is similarly plotted, and one readily observes that their runtimes are essentially identical. The runtime of Alg. 4 for arbitrary, complex, non-Hermitian marginal kernels is similarly shown in Fig. 6. For purpose of comparison, we note that the double-precision High-Performance LINPACK benchmark [43] achieves roughly 1 TFlop/second on this machine.

It is worth emphasizing the compounding performance gains from both the formulation of DPP sampling as a small modification of a level-3 BLAS focused dense matrix factorization and from the 16-way parallelism. When combined, a factor of 2500x speedup is observed relative to the timings on the same machine of DPPy v0.1.0 [44] when sampling a spectrally-preprocessed arbitrary, dense Hermitian  $5000 \times 5000$  matrix. Similar speedups exist relative to the timings of both the “sequentially thinned” and spectrally-preprocessed algorithms of [3]. In the case of DPPy, it would be fair to attribute at least an order of magnitude of the performance difference to its implementation being standard Python code rather than optimized C++.

In the case of DPPs where the expected number of samples,  $k \equiv \text{trace}(K)$ , is much less than the ground set size,  $n$ , Derezhinski et al. [45] have proposed a rejection-sampling approach with a setup cost of  $n \cdot \text{polylog}(n) \cdot \text{poly}(k)$  and a subsequent sampling cost of  $\text{poly}(k)$ . Ignoring polylogarithmic terms,

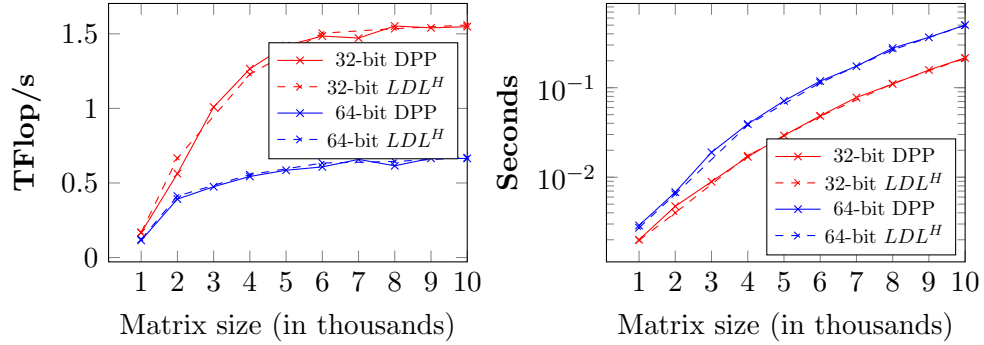


Figure 5: Dense, real  $LDL^H$ -based DPP sampling performance; tile sizes of 128 and 256 were used for matrix sizes less than or equal to, and greater than, 2000, respectively.

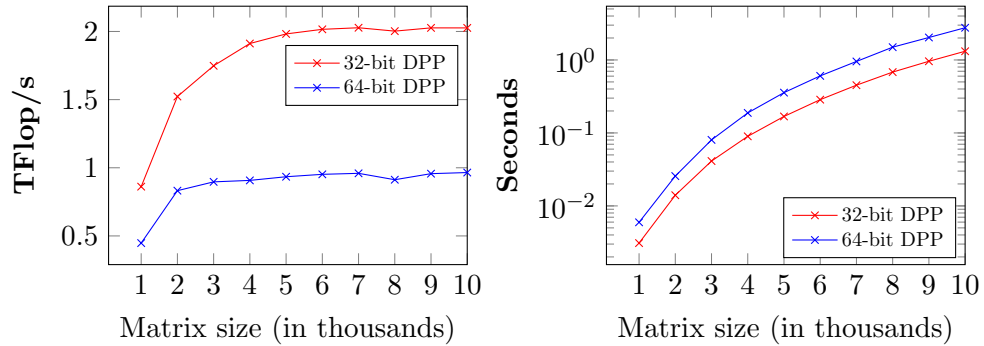


Figure 6: Dense, complex  $LU$ -based DPP sampling performance. For single-precision, a tile size of 128 was used up to matrix sizes of 3000, and tile sizes of 256 were used thereafter. For double-precision, the switch occurred above matrices of size 4000.

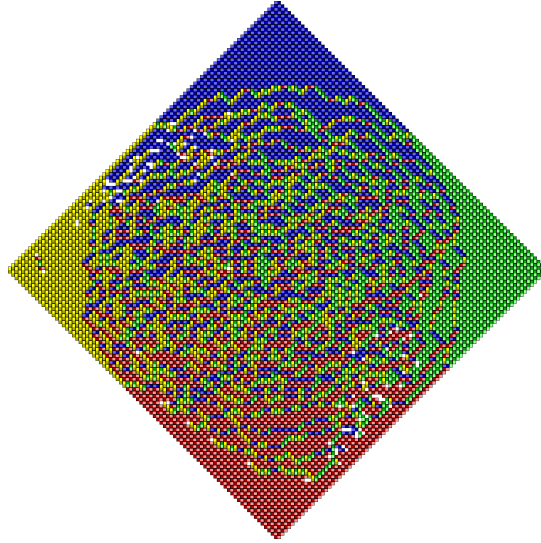


Figure 7: Corrupted single-precision sample from an Aztec diamond of size 80. Missing tiles are clearly visible in the image.

their setup cost is  $O(nk^6 + k^9)$  and the subsequent sampling cost is  $O(k^6)$ . Large speedups can therefore be expected when  $k \ll \sqrt{n}$ . But the examples in Figs. 1–4 of this article all involve  $k$  being a modest fraction of  $n$ , e.g.,  $k \approx n/4$  in the case of the Aztec diamond, so the rejection sampler would involve a prohibitive  $O(n^9)$  setup and  $O(n^6)$  subsequent sampling cost.

Timings for the  $\mathbb{Z}^2$  and hexagonal-tiling Uniform Spanning Tree DPPs can be extracted from Fig. 5 via the formulae  $n \approx 2d^2$  and  $n \approx 6d^2$ , respectively, where  $d$  is the order of the grid. And timings for the uniform domino tilings can be recovered from Fig. 6 via the formula  $n \approx 4d^2$ . When computing results for the latter, it was noticed that sampling domino tilings from the Kenyon formula DPP in single-precision, the results are essentially always inconsistent once the diamond size exceeds 60, but no inconsistencies have yet been observed with double-precision sampling. See Fig. 7 for an example.

Such a numerical instability in an unpivoted dense matrix factorization would lead any numerical analyst to wonder if dynamic pivoting can mitigate error accumulation. Indeed, our factorization-based approach frees us to perform arbitrary diagonal pivoting, as long as the pivot is decided before its corresponding Bernoulli draw. While it will be the subject of future work, the author conjectures that *maximum-entropy* pivoting, that is, piv-

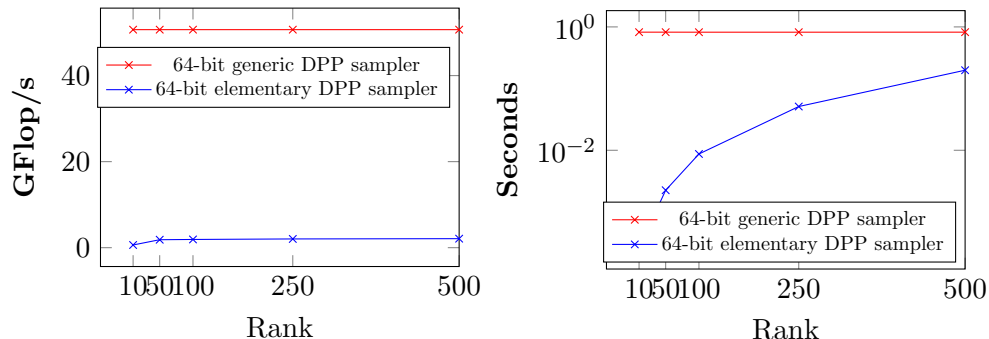


Figure 8: Sequential, dense, real  $LDL^H$ -based elementary DPP sampling performance for a ground set of size 5000 and varying rank. Multithreaded BLAS was explicitly disabled to ensure execution on a single core of the Intel i9-7960x.

oting towards a diagonal entry with conditional probability as close to  $\frac{1}{2}$  as possible, would be the most beneficial, as it maximizes the magnitude of the smallest possible pivot.

Before moving on to sparse-direct DPP sampling, we demonstrate the multiple orders of magnitude speedup that are possible for Determinantal Projection Processes of sufficiently low rank. Unlike our other experiments, Fig. 8 only executes on a single core, as the unblocked, left-looking rank-revealing elementary DPP sampling approach of Alg. 2 spends the majority of its time in matrix/vector multiplication. Studying the benefits of parallelizations of elementary DPP samplers is left for future work.

## 4 Sparse-direct DPP sampling

As was demonstrated in Fig. 5, the performance of a generic Hermitian DPP sampler can be made to match that of a high-performance Hermitian matrix factorization. This correspondence should not be a surprise, as we have shown that matrix factorizations can be trivially modified to yield Hermitian and non-Hermitian DPP samplers alike. The same insight applies to the conversion of sparse-direct, unpivoted  $LDL^H$  factorization into sparse-direct Hermitian DPP samplers. Such an implementation, mirroring many of the techniques from CholMod [33], was implemented within Catamari.

The high-level approach is to use a dynamically scheduled – via OpenMP 4.0 task scheduling – *multifrontal method* [46, 32] when the computational intensity of the factorization is deemed high enough after determining the

number of nonzeros and of the triangular factor and the number of operations required to compute it. If the arithmetic count and intensity is not sufficiently high, an *up-looking*, scalar algorithm [33] is used instead.

The multifrontal method performs the bulk of its work processing an (*elimination*) tree of dense *frontal matrices* in a post-ordering. Each such frontal matrix for a supernode  $s$  initially takes the form

$$\begin{pmatrix} A_s & * \\ A_{\text{struct}(s),s} & 0 \end{pmatrix},$$

where  $A_s$  is the diagonal block of the input matrix corresponding to supernode  $s$ ,  $A_{\text{struct}(s),s}$  is the submatrix of  $A$  below the supernodal diagonal block that contains at least one nonzero in each row, and the  $*$  denotes the upper-right quadrant not needing to be accessed due to Hermiticity. Processing such a front involves adding any child Schur complements onto the front, factoring  $A_s = L_s D_s L_s^H$ , solving against  $D_s L_s^H$  to replace  $A_{\text{struct}(s),s}$  with  $L_{\text{struct}(s),s}$ , and replacing the bottom-right quadrant with the Schur complement  $-L_{\text{struct}(s),s} D_s L_{\text{struct}(s),s}^H$ .

This multifrontal process is then parallelized using a tile-based, dynamically scheduled DPP sampler or dense factorization on the diagonal blocks, combined with nested OpenMP tasks launched for each (relaxed) supernode’s [32] subtree [47].

While the author is not aware of any well-studied sparse marginal kernel matrices, [48] proposed a scheme for learning data-sparse marginal kernels defined via Kronecker products and evaluated their technique on the Amazon baby registry dataset of [49]. While DPP learning schemes are beyond the scope of this manuscript, the dramatic factorization speedups that can be supplied by sparse-direct solvers suggests the possibility of learning an entrywise sparse marginal kernel matrix, perhaps via incorporating entrywise soft-thresholding into an iterative learning scheme [49].

We therefore implemented tandem sparse-direct factorization and sparse-direct Hermitian DPP samplers to connect performance results of synthetic sparse DPPs and discretized Partial Differential Equation solvers. Such a statically-pivoted sparse-direct  $LDL^H$  factorization is also the critical computational kernel of primal-dual Interior Point Methods [50, 51], where the first-order optimality conditions are symmetric quasi-semidefinite [52, 53].

Performance results for the dynamically scheduled sparse-direct solver on a 3D Helmholtz equation discretized with trilinear, hexahedral elements Fig. 9 are shown in Fig. 10; results for a 2D DPP analogue, where the marginal kernel takes the form of a scaled 2D Laplacian, are shown in Fig. 11.

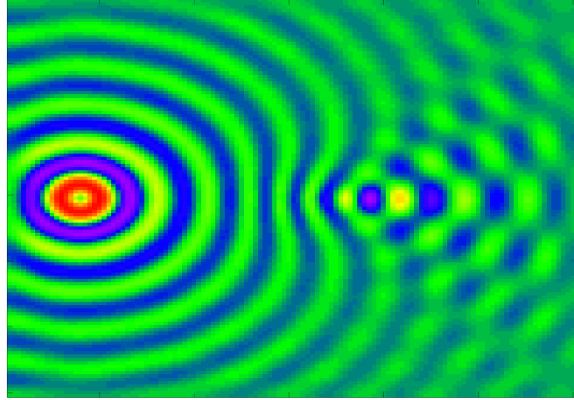


Figure 9: A 2D slice for a solution of a 3D Helmholtz equation discretized with trilinear, hexahedra elements and PML boundary conditions for a Gaussian point source near the boundary and a converging lens near the center of the domain.

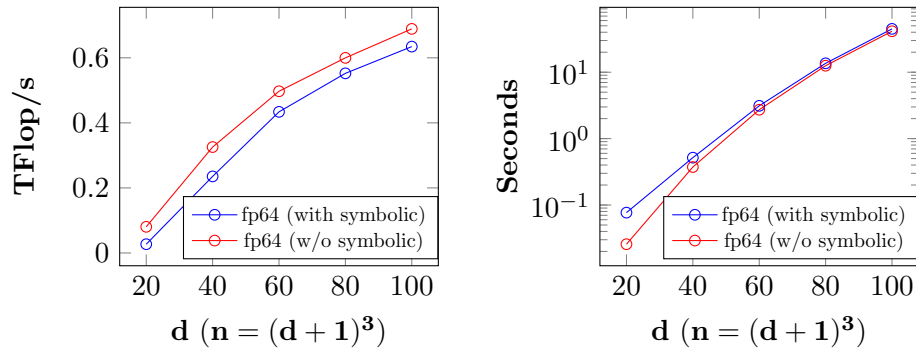
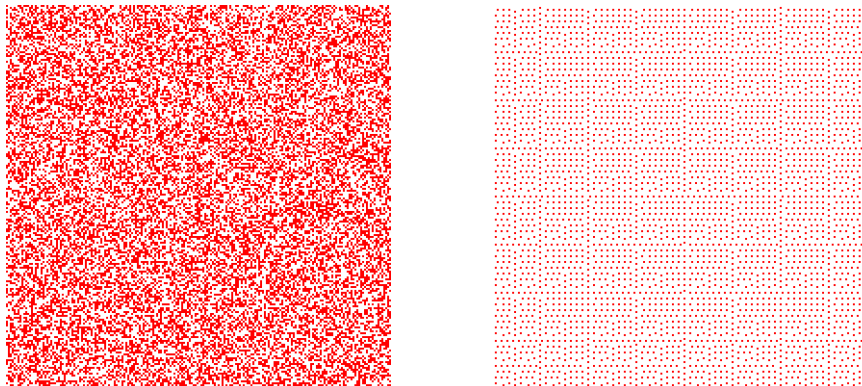


Figure 10: Sparse-direct performance on trilinear, hexahedral discretization of 3D Helmholtz equation with Perfectly Matched Layer boundary conditions.



(a) Sample with log-likelihood of -27472.2. (b) Greedy maximum-likelihood sample with log-likelihood of -26058.

Figure 11: Samples from  $-\sigma\Delta$  over a 200 x 200 grid, where  $\sigma = 0.72$ .

In the case of the 2D Laplacian sparse-direct DPP sampling over a  $200 \times 200$  grid, the timings were roughly 0.01 seconds on the 16-core i9-7960x. Extrapolating from Fig. 5 to a dense matrix size of 40,000, it is clear that several more orders of magnitude of efficiency are gained with the sparse-direct formulation.

We close this section by noting that static pivoting should apply equally well to non-Hermitian sparse-direct DPP sampling, as the nature of small pivots being, by definition, rare, suggests a certain degree of stability. As in the case of dense DPP sampling, probabilistic error analysis is warranted.

## 5 Conclusions

A unified, generic framework for sequentially sampling both Hermitian and non-Hermitian Determinantal Point Processes directly from their marginal kernel matrices was presented. The prototype algorithm consisted of a small modification of an unpivoted LU factorization – in the Hermitian case, it reduces to a modification of an unpivoted  $LDL^H$  factorization – and high-performance, tiled algorithms were presented in the dense case, and an analogue of CholMod [33] was presented for the sparse case. Further, it was shown that both greedy, maximum-likelihood sampling and elementary DPP sampling can be understood and efficiently implemented using small modifications of traditional matrix factorization techniques.

In addition to generalizing sampling algorithms from Hermitian to non-

Hermitian marginal kernels, the proposed approaches were implemented within the open source, permissively licensed, Catamari package and shown to lead to orders of magnitude speedups, even in the dense regime. The Hermitian sparse-direct DPP sampler leads to further asymptotic speedups. Future work includes theoretical and empirical exploration of the stability of dynamic pivoting techniques, both for dense and sparse-direct factorization-based DPP sampling, including the incorporation of maximum-entropy pivoting for large instances of Kenyon-formula Aztec domino tilings.

Further exploration of the performance tradeoffs between left-looking and right-looking elementary DPP sampling, and at which rank it becomes beneficial to use our generic sampling approach, is warranted – especially on multi-core and GPU-accelerated architectures. And, lastly, the incorporation of a tiled extension of [54] for converting a Hermitian L-ensemble kernel into a marginal kernel via  $K = I - (L + I)^{-1}$  [25] is a natural extension of our proposed techniques and could be expected to require the equivalent of 3 samples worth of time due to the computational complexity.

But perhaps the most pressing future direction is to investigate the potential of learning sparse marginal kernels on a benchmark problem, such as the Amazon baby registry of [49]. Ideally such a scheme would expose a roughly block-diagonal covariance matrix which captures item clusters and allows for sufficiently sparse triangular factors.

## Reproducibility

The experiments in this paper were performed using version 0.2.5 of Catamari, with Intel’s Math Kernel Library BLAS on an Ubuntu 18.04 workstation with 64 GB of RAM and an Intel i9-7960x processor. Catamari can be downloaded from [https://gitlab.com/hodge\\_star/catamari](https://gitlab.com/hodge_star/catamari). Figs. 1 and 2 were generated using the TIFF output from example driver `example/uniform_spanning_tree.cc`, while Figs. 3, 4 and 7 similarly used `example/aztec_diamond.cc`.

Figs. 5 and 6 were generated using data from `example/dense_dpp.cc` and `example/dense_factorization.cc`; we emphasize that explicitly setting both `OMP_NUM_THREADS` and `MKL_NUM_THREADS` to 16 on our 16-core machine led to significant performance improvements (as opposed to the default exploitation of hyperthreading). And Fig. 8 was produced with `example/dense_elementary_dpp.cc` – with `OMP_NUM_THREADS` and `MKL_NUM_THREADS` explicitly set to one. The algorithmic `block_size` was also set to a value at least as large as the rank so that a left-looking approach

was used throughout.

Figs. 9 and 10 were generated from `example/helmholtz_3d_pml.cc`, with the 2D-slice of the former taken slightly away from the center plane. Fig. 11 was output from the TIFF support of `example/dpp_shifted_2d_negative_laplacian.cc`.

## Acknowledgements

The author would like to sincerely thank Guillaume Gautier and Rémi Bardenet for detailed comments on an early draft of this manuscript, as well as their concise explanation of the correctness of the factorization-based sampler at [https://dppy.readthedocs.io/en/latest/finite\\_dpps/exact\\_sampling.html#id17](https://dppy.readthedocs.io/en/latest/finite_dpps/exact_sampling.html#id17). I would also like to thank Jennifer A. Gillenwater for suggesting the  $I - (L + I)^{-1}$  conversion from an L-ensemble and Alex Kulesza for answering some of my early DPP questions. Lastly, I am thankful for the insightful comments and suggestions of the two anonymous referees: they significantly improved the quality of the manuscript.

## References

- [1] Odile Macchi. The coincidence approach to stochastic point processes. *Advances in Applied Probability*, 7(1):83–122, 1975.
- [2] Alex Kulesza and Ben Taskar. Determinantal point processes for machine learning. *Foundations and Trends in Machine Learning*, 5(2–3):123–286, 2012.
- [3] Claire Launay, Bruno Galerne, and Agnès Desolneux. Exact Sampling of Determinantal Point Processes without Eigendecomposition. *arXiv e-prints*, page arXiv:1802.08429, Feb 2018.
- [4] Laming Chen and Guoxin Zhang. Fast greedy map inference for determinantal point process to improve recommendation diversity. In *NeurIPS*, 2018.
- [5] Odile Macchi. *The Fermion Process — A Model of Stochastic Point Process with Repulsive Points*, pages 391–398. Springer Netherlands, Dordrecht, 1977.

- [6] Madan L. Mehta and Michel Gaudin. On the density of eigenvalues of a random matrix. *Nuclear Physics*, 18:420–427, 1960.
- [7] Freeman J. Dyson. Statistical theory of the energy levels of complex systems. i. *Journal of Mathematical Physics*, 3(1):140–156, 1962.
- [8] Freeman J. Dyson. Statistical theory of the energy levels of complex systems. ii. *Journal of Mathematical Physics*, 3(1):157–165, 1962.
- [9] Freeman J. Dyson. Statistical theory of the energy levels of complex systems. iii. *Journal of Mathematical Physics*, 3(1):166–175, 1962.
- [10] Jean Ginibre. Statistical Ensembles of Complex, Quaternion and Real Matrices. *J. Math. Phys.*, 6:440–449, 1965.
- [11] Persi Diaconis. Patterns in eigenvalues: the 70th Josiah Willard Gibbs lecture. *Bull. Amer. Math. Soc.*, 40:155–178, 2003.
- [12] Alan Edelman and N. Raj Rao. Random matrix theory. *Acta Numerica*, 14:233–297, 2005.
- [13] Robert Burton and Robin Pemantle. Local characteristics, entropy and limit theorems for spanning trees and domino tilings via transfer-impedances. *The Annals of Probability*, 21(3):1329–1371, 1993.
- [14] Itai Benjamini, Russell Lyons, Yuval Peres, and Oded Schramm. Uniform spanning forests. *Ann. Probab.*, 29(1):1–65, 02 2001.
- [15] Kurt Johansson. Determinantal processes with number variance saturation. *Communications in Mathematical Physics*, 252(1):111–148, Dec 2004.
- [16] Peter W. Kasteleyn. The statistics of dimers on a lattice : I. The number of dimer arrangements on a quadratic lattice. *Physica*, 27:1209–1225, December 1961.
- [17] Harold N. V. Temperley and Michael E. Fisher. Dimer problem in statistical mechanics-an exact result. *The Philosophical Magazine: A Journal of Theoretical Experimental and Applied Physics*, 6(68):1061–1063, 1961.
- [18] Peter W. Kasteleyn. Dimer statistics and phase transitions. *Journal of Mathematical Physics*, 4(2):287–293, 1963.

- [19] Sunil Chhita, Kurt Johansson, and Benjamin Young. Asymptotic domino statistics in the aztec diamond. *Ann. Appl. Probab.*, 25(3):1232–1278, 06 2015.
- [20] Persi Diaconis and Steven N. Evans. Immanants and finite point processes. *Journal of Combinatorial Theory, Series A*, 91(1):305–321, 2000.
- [21] William Jockusch, James Propp, and Peter Shor. Random Domino Tilings and the Arctic Circle Theorem. *arXiv Mathematics e-prints*, page math/9801068, Jan 1998.
- [22] Victor-Emmanuel Brunel. Learning signed determinantal point processes through the principal minor assignment problem. In S. Bengio, H. Wallach, H. Larochelle, K. Grauman, N. Cesa-Bianchi, and R. Garnett, editors, *Advances in Neural Information Processing Systems 31*, pages 7365–7374. Curran Associates, Inc., 2018.
- [23] Alexander Soshnikov. Determinantal random point fields. *Russian Mathematical Surveys*, 55(5):923–975, oct 2000.
- [24] J. Ben Hough, Manjunath Krishnapur, Yuval Peres, and Balint Virag. Determinantal processes and independence. *Probab. Surveys*, 3:206–229, 2006.
- [25] Jennifer A. Gillenwater. *Approximate Inference for Determinantal Point Processes*. PhD thesis, University of Pennsylvania, 2014.
- [26] Nicholas J. Higham. Analysis of the Cholesky decomposition of a semi-definite matrix. In *Reliable Numerical Computation*, pages 161–185. University Press, 1990.
- [27] Mike Gartrell, Victor-Emmanuel Brunel, Elvis Dohmatob, and Syrine Krichene. Learning nonsymmetric determinantal point processes. *CoRR*, abs/1905.12962, 2019.
- [28] Edward Anderson, Zhaojun Bai, Jack J. Dongarra, Anne Greenbaum, Alan McKenney, Jeremy Du Croz, Sven Hammarling, James Demmel, Christian Bischof, and Danny Sorensen. LAPACK: A portable linear algebra library for high-performance computers. In *Proceedings of the 1990 ACM/IEEE Conference on Supercomputing*, Supercomputing '90, pages 2–11, Los Alamitos, CA, USA, 1990. IEEE Computer Society Press.

- [29] Ernie Chan, Field G. Van Zee, Paolo Bientinesi, Enrique S. Quintana-Orti, Gregorio Quintana-Orti, and Robert van de Geijn. SuperMatrix: A multithreaded runtime scheduling system for algorithms-by-blocks. In *Proceedings of the 13th ACM SIGPLAN Symposium on Principles and Practice of Parallel Programming*, PPOPP '08, pages 123–132, New York, NY, USA, 2008. ACM.
- [30] Alfredo Buttari, Julien Langou, Jakub Kurzak, and Jack Dongarra. A class of parallel tiled linear algebra algorithms for multicore architectures. *Parallel Comput.*, 35(1):38–53, January 2009.
- [31] Robert Schreiber. A new implementation of sparse Gaussian elimination. *ACM Trans. Math. Softw.*, 8(3):256–276, September 1982.
- [32] Cleve Ashcraft and Roger Grimes. The influence of relaxed supernode partitions on the multifrontal method. *ACM Trans. Math. Softw.*, 15(4):291–309, December 1989.
- [33] Yanqing Chen, Timothy A. Davis, William W. Hager, and Sivasankaran Rajamanickam. Algorithm 887: Cholmod, supernodal sparse cholesky factorization and update/downdate. *ACM Trans. Math. Softw.*, 35(3):22:1–22:14, October 2008.
- [34] Inderjit S. Dhillon, Beresford N. Parlett, and Christof Vömel. The design and implementation of the mrrr algorithm. *ACM Trans. Math. Softw.*, 32(4):533–560, December 2006.
- [35] Bruce Hendrickson, Elizabeth Jessup, and Christopher Smith. Toward an efficient parallel eigensolver for dense symmetric matrices. *SIAM J. Sci. Comput.*, 20(3):1132–1154, January 1999.
- [36] Christian H. Bischof, Bruno Lang, and Xiaobai Sun. A framework for symmetric band reduction. *ACM Trans. Math. Softw.*, 26(4):581–601, December 2000.
- [37] Azzam Haidar, Hatem Ltaief, and Jack Dongarra. Parallel reduction to condensed forms for symmetric eigenvalue problems using aggregated fine-grained and memory-aware kernels. In *Proceedings of 2011 International Conference for High Performance Computing, Networking, Storage and Analysis*, SC '11, pages 8:1–8:11, New York, NY, USA, 2011. ACM.

- [38] Grey Ballard, James Demmel, and Nicholas Knight. Avoiding communication in successive band reduction. *ACM Trans. Parallel Comput.*, 1(2):11:1–11:37, February 2015.
- [39] Charles L. Lawson, Richard J. Hanson, Fred T. Krogh, and David R. Kincaid. Algorithm 539: Basic Linear Algebra Subprograms for Fortran usage [F1]. *ACM Trans. Math. Softw.*, 5(3):324–325, September 1979.
- [40] Jack J. Dongarra, Jeremy Du Croz, Sven Hammarling, and Richard J. Hanson. An extended set of FORTRAN Basic Linear Algebra Subprograms. *ACM Trans. Math. Softw.*, 14(1):1–17, March 1988.
- [41] Jack J. Dongarra, Jeremy Du Croz, Sven Hammarling, and I. S. Duff. A set of level 3 Basic Linear Algebra Subprograms. *ACM Trans. Math. Softw.*, 16(1):1–17, March 1990.
- [42] OpenMP Architecture Review Board. OpenMP application program interface version 4.0, 2013.
- [43] Jack J. Dongarra, Piotr Luszczek, and Antoine Petit. The LINPACK benchmark: Past, present, and future, 2002.
- [44] Guillaume Gautier, Rémi Bardenet, and Michal Valko. DPPy: Sampling determinantal point processes with Python. *CoRR*, abs/1809.07258, 2018.
- [45] Michal Dereziński, Daniele Calandriello, and Michal Valko. Exact sampling of determinantal point processes with sublinear time preprocessing. *CoRR*, abs/1905.13476, 2019.
- [46] Iain S. Duff and John K. Reid. The multifrontal solution of indefinite sparse symmetric linear. *ACM Trans. Math. Softw.*, 9(3):302–325, September 1983.
- [47] Jonathan Hogg and Jennifer Scott. New parallel sparse direct solvers for multicore architectures. *Algorithms*, 6(4):702–725, 2013.
- [48] Zelda Mariet and Suvrit Sra. Kronecker determinantal point processes. *CoRR*, abs/1605.08374, 2016.
- [49] Jennifer Gillenwater, Alex Kulesza, Emily Fox, and Ben Taskar. Expectation-maximization for learning determinantal point processes. In *Proceedings of the 27th International Conference on Neural Information Processing Systems - Volume 2*, NIPS’14, pages 3149–3157, Cambridge, MA, USA, 2014. MIT Press.

- [50] Anna Altman and Jacek Gondzio. HOPDM – a higher order primal-dual method for large scale linear programming. *European Journal of Operational Research*, 66(1):158 – 160, 1993.
- [51] Jacek Gondzio. Multiple centrality corrections in a primal-dual method for linear programming. *Computational Optimization and Applications*, 6(2):137–156, Sep 1996.
- [52] Robert Vanderbei. Symmetric quasidefinite matrices. *SIAM Journal on Optimization*, 5(1):100–113, 1995.
- [53] Alan George, Khakim Ikramov, and Andrey B. Kucherov. Some properties of symmetric quasi-definite matrices. *SIAM Journal on Matrix Analysis and Applications*, 21(4):1318–1323, 2000.
- [54] Paolo Bientinesi, Brian Gunter, and Robert A. van de Geijn. Families of algorithms related to the inversion of a symmetric positive definite matrix. *ACM Trans. Math. Softw.*, 35(1):3:1–3:22, July 2008.